

FINITE TEMPERATURE DYNAMICS NEAR QUANTUM PHASE TRANSITIONS

SUBIR SACHDEV

*Department of Physics, Yale University,
P.O. Box 208120, New Haven, CT 06520-8120, USA.
E-mail: subir.sachdev@yale.edu*

We review the non-zero temperature relaxational dynamics of quantum systems near a zero temperature, second-order phase transition. We begin with the quantum Ising chain, for which universal and exact results for the relaxation rates can be obtained in all the distinct limiting regimes of the phase diagram. Next, we describe the crossovers in the electron spectral function near a transition involving a change in the pairing symmetry of BCS superconductors in two dimensions. Finally, we consider dynamic spin models which may provide a mean-field description of magnetic ordering transitions in the heavy fermion compounds.

Keynote talk at the 11th International Conference on
Recent Progress in Many-Body Theories,
UMIST, Manchester UK, 9-13 July, 2001

1 Introduction

The description of the long-time, low temperature, collective dynamics of condensed matter systems is one of the central aims of quantum many body theory.^{1,2,3} Numerous successful theories have been developed for a variety of materials, and we can broadly separate them into two (not entirely distinct) categories:

Order parameter dynamics: Often the system is in or near a phase with a broken symmetry. This can be used to define an order parameter which, along with globally conserved quantities, obey equations of motion which define the collective, long-time dynamics. The simplest example of this was the van Hove theory, which evolved into a sophisticated description of the highly non-trivial dynamics near finite temperature second order phase transitions.⁴

Quasiparticle dynamics: The elementary excitations above a particular ground states are identified, and a transport equation for their collision and interactions provides a description of the low frequency response functions. Landau's Fermi liquid theory³ is the familiar example of such a theory.

One common feature of both classes of models is that the dynamic equations controlling the lowest frequency dynamics are ultimately *classical*. They do, nevertheless, provide a description of quantum systems at low temperature. Quantum mechanics does play a fundamental role in determining the nature of the ground state, its excitations, and of effective coupling constants in the equations of motion, but the equations are finally expressed in terms of classical, collective degrees of freedom. For the order parameter dynamics, the justification for a classical description is that the typical relaxation frequency is smaller than $k_B T / \hbar$ (where T is the absolute temperature), while in the quasiparticle models we require a collision frequency smaller than $k_B T / \hbar$.

In this paper, we will review recent studies of finite temperature dynamics near second-order quantum phase transitions.⁵ We will find that the two classes of classical models discussed above do apply over a significant portion of the phase diagram. However, we will also discuss the novel *quantum critical* region,⁶ where both descriptions are inadequate. The fundamental property of this region^{7,8} is that the characteristic frequency is a number of order unity (which is usually universal) times $k_B T/\hbar$: so neither classical description is evidently applicable. A theory of quantum-critical dynamics can, of course, be obtained from an exact solution of the critical field theory describing the phase transition: we will see an example of this in Section 2 and the results yield considerable insight. However, such exact solutions are rare, and cannot be relied upon for a general theory. Various perturbative approaches to quantum critical dynamics have been developed,^{9,10} and these usually rely upon effective classical models of order-parameter or quasiparticle dynamics as a point of departure.

We will begin our discussion in Section 2 by considering the quantum Ising chain. An essentially exact description of the long time dynamics is available¹¹ in all the different low temperature regions of the phase diagram of this model, and this will allow us to describe and distinguish the essential characteristics of the order-parameter, quasiparticle, and quantum-critical dynamics. Section 3 will consider a quantum critical point in two dimensions between two superconductors with distinct pairing symmetries. The critical theory involves interacting fermionic and bosonic excitations, and we will discuss approximate theories for the quantum critical dynamics and their possible relevance to recent photo-emission experiments on the cuprate superconductors. Finally, in Section 4 we will discuss the quantum critical dynamics in simplified models of correlated electrons in the presence of quenched disorder, and their relationship to experiments on the heavy fermion superconductors.

The reader is also referred to another recent review¹² which covers additional topics on quantum phase transitions presented in my talk at MB-11.

2 Quantum Ising chain

We consider one of the simplest models which displays a second-order quantum phase transitions; its phase diagram is nevertheless rich enough to display all the dynamic regimes we wish to distinguish. The Hamiltonian of the quantum Ising chain is

$$H_I = - \sum_j \left(\sum_{\ell>0} J_\ell \sigma_j^z \sigma_{j+\ell}^z + g \sigma_j^x \right) \quad (1)$$

where σ_j^z, σ_j^x are Pauli matrices on a chain of sites j , $J_\ell (> 0)$ are short-ranged exchange constants, and $g (> 0)$ is the transverse field. The operator $\prod_j \sigma_j^x$ commutes with H_I , and generates its global Z_2 Ising symmetry. We will consider the phase diagram¹¹ of H_I as a function of g and T , shown in Fig 1. The global Z_2 symmetry is spontaneously broken at $T = 0$ for $g < g_c$, where g_c is a critical value of order the J_ℓ . There is a second order phase transition at $g = g_c, T = 0$, and the

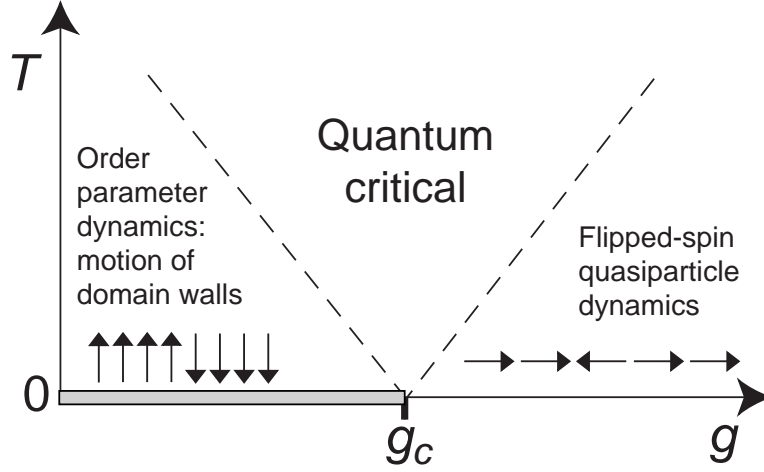


Figure 1. Phase diagram of the quantum Ising chain H_I in (1). There is long range order, with $N_0 \neq 0$ in (3), only for $g < g_c$ and $T = 0$ on the shaded line. The dashed lines represent crossovers at $\Delta \sim k_B T$. Quasiclassical models for the long times dynamics in the lower left (Section 2.1) and lower right (Section 2.2) regions are available. The quantum critical dynamics is discussed in Section 2.3.

symmetry is restored elsewhere in the phase diagram. We describe the different regimes of Fig 1 in the following subsections.

2.1 Order parameter dynamics

First consider H_I at $g = 0$. Here H_I is the classical Ising model and all states are known exactly, as is the $T > 0$ partition function. The ground states are doubly degenerate, $\prod_j |\uparrow\rangle_j$ or $\prod_j |\downarrow\rangle_j$, and have long-range ferromagnetic order in σ_j^z . All excited states can also be written down exactly, and the lowest energy ones are domain walls between the two ordered states

$$\dots |\uparrow\rangle_{j-2} |\uparrow\rangle_{j-1} |\uparrow\rangle_j |\downarrow\rangle_{j+1} |\downarrow\rangle_{j+2} |\downarrow\rangle_{j+3} \dots, \quad (2)$$

whose energy is $\Delta = 2 \sum_{\ell > 0} \ell J_\ell$ above the ground state. The entire set of excited states can be built out of multiple domain wall states. At a small $T > 0$, there is an exponentially small density $\rho \sim e^{-\Delta/k_B T}$ of thermally excited domain walls. A simple calculation shows that the presence of these excitations is sufficient to destroy the long range order beyond an exponentially large correlation length $\xi = 1/2\rho$.

Now move to a small $g > 0$. All the states are now perturbed by quantum fluctuations, but the qualitative picture remains the same at long length scales. There is still ferromagnetic order in the ground state, and a broken Z_2 symmetry, with the long range correlation

$$\lim_{|j-k| \rightarrow \infty} \langle \sigma_j^z \sigma_k^z \rangle_{T=0} = N_0^2, \quad (3)$$

but N_0 is no longer unity as it is in the classical model; instead quantum fluctuations reduce N_0 with increasing g until it ultimately vanishes at $g = g_c$. This subsection

will restrict attention to $g < g_c$. The degenerate manifold of the domain wall states (2) now broaden into a band of single particle states with dispersion $\varepsilon_p = \Delta + 4g \sin^2(p/2) + \mathcal{O}(g^2)$ as function of momentum p ; we assume unit lattice spacing) and have now redefined Δ to be the true energy gap including all corrections. The resulting motion and collision of the thermally excited domain walls is responsible for the long time relaxational dynamics of the ferromagnetic order parameter. This picture was used to develop a simple solvable quasiclassical theory¹¹ for the dynamic correlations of the order parameter in the $g < g_c$, low T region of Fig 1, and the results are most conveniently expressed in terms of the dynamic structure factor $S(p, \omega)$:

$$S(p, \omega) = \sum_j \int_{-\infty}^{\infty} dt e^{-i(pj - \omega t)} \text{Tr} \left(e^{-H_I/k_B T} e^{iH_I t/\hbar} \sigma_j^z e^{-iH_I t/\hbar} \sigma_0^z \right) / \text{Tr} \left(e^{-H_I/k_B T} \right) \quad (4)$$

At $T = 0$, the long-range order (3) leads to the elastic Bragg peak

$$S(p, \omega) = (2\pi)^2 N_0^2 \delta(p) \delta(\omega) + \dots \quad (5)$$

where the ellipsis represents contributions at frequencies $\omega > 2\Delta$ associated with the creation of two or more domain walls by the external probe. At $T > 0$ the quasiclassical order parameter dynamics broadens the delta functions in (5), and leads to

$$S(p, \omega) = N_0^2 \int_{-\infty}^{\infty} dx \int_{-\infty}^{\infty} dt e^{-i(px - \omega t)} R(x, t) + \dots \quad (6)$$

where $R(x, t)$ is a relaxational function. The form of $R(x, t)$ for general x, t is involved, but its basic features can be understood by looking at two simple limits:

$$\begin{aligned} R(x, 0) &= e^{-|x|/\xi} \quad ; \quad \frac{1}{\xi} = 2 \int_{-\pi}^{\pi} \frac{dp}{2\pi} e^{-\varepsilon_p/k_B T} \\ R(0, t) &= e^{-|t|/\tau_\varphi} \quad ; \quad \frac{1}{\tau_\varphi} = \frac{2k_B T}{\pi\hbar} e^{-\Delta/k_B T}. \end{aligned} \quad (7)$$

So R decays exponentially on a characteristic spatial scale ξ , and a characteristic temporal scale, the coherence time τ_φ ; the delta functions in (5) therefore broaden at $T > 0$ to a momentum width of order $1/\xi$, and a frequency width of order $1/\tau_\varphi$. The expression (7) contains an exact result for τ_φ at low T : the quantum Ising chain, and the closely related dilute Bose gas,^{13,11} are the only interacting many body quantum systems for which exact results for such a relaxation rate are available. Remarkably, τ_φ involves only the energy gap Δ and fundamental constants of nature; it also satisfies $\tau_\varphi \gg \hbar/k_B T$ as is required for the applicability of the quasiclassical theory.

2.2 Quasiparticle dynamics

Next consider the opposite limit of very large g . At $g = \infty$ all eigenstates can again be written down simply. There is a unique, paramagnetic ground state $\prod_j |\rightarrow\rangle_j$, where $|\rightarrow\rangle_j = (|\uparrow\rangle_j + |\downarrow\rangle_j)/\sqrt{2}$ is an eigenstate of σ_j^x . In strong contrast to the states at $g = 0$, equal time correlations of σ_j^z are now non-zero only on-site, and so

the spin correlation length is effectively zero. The lowest excited states are obtained by flipping a single spin:

$$\dots |\rightarrow\rangle_{j-2} |\rightarrow\rangle_{j-1} |\leftarrow\rangle_j |\rightarrow\rangle_{j+1} |\rightarrow\rangle_{j+2} |\rightarrow\rangle_{j+3} \dots, \quad (8)$$

where $|\leftarrow\rangle_j = (|\uparrow\rangle_j - |\downarrow\rangle_j)/\sqrt{2}$ is the other eigenstate of σ_j^x , and these states have energy $2g$ above the ground state. We can now examine corrections to the limit case in powers of $1/g$. The ground state remains paramagnetic but the spin correlation length increases as g is decreased. The flipped spin states (8) again broaden into a quasiparticle band with $\varepsilon_p = \Delta + 4 \sum_{\ell>0} J_\ell \sin^2(p\ell/2) + \mathcal{O}(g^2)$ and $\Delta = 2g - 2 \sum_{\ell>0} J_\ell + \mathcal{O}(g^2)$. Keep in mind, however, that the physical interpretation of these quasiparticles is entirely distinct from those of Section 2.1: they are not domain walls, but localized spin flips. A crucial property of the quasiparticles is that they have an infinite lifetime for a finite range of momenta around $p = 0$: this is simply because energy and momentum conservation prohibit their decay into any other states. Consequently, although equal time correlations of σ_j^z decay very rapidly in space, there are long-range correlations in spacetime; this is evident from the expression for the dynamic structure factor

$$S(p, \omega) = \pi \mathcal{A} \delta(\omega - \varepsilon_p/\hbar) + \dots \quad ; \quad T = 0, \quad (9)$$

associated with quasiparticle pole, as infinite range temporal and spatial correlations are needed for the Fourier transform to conspire to have a pole. Here the ellipsis represents multiparticle contributions at frequencies $\omega > 3\Delta$. The quasi-particle residue \mathcal{A} is finite in the paramagnetic phase and decreases as g is decreased.

At $T > 0$, there will again be an exponentially small density of these thermally excited quasiparticles. A quasiclassical transport equation for the collisions of these quasiparticles can be written down and, remarkably, solved exactly. This solution shows that the quasiparticle collisions broaden (9) into a Lorentzian

$$S(p, \omega) = \frac{\mathcal{A}/\tau_\varphi}{(\omega - \varepsilon_p/\hbar)^2 + (1/\tau_\varphi)^2}. \quad (10)$$

The expression for the quasiparticle-width, $1/\tau_\varphi$, turns out to be identical to that in (7), where Δ is now the energy gap to the flipped-spin quasiparticles. Note that the characteristic collision time is again larger than $\hbar/k_B T$, as is needed to justify a classical dynamical model.

2.3 Quantum critical dynamics

The quasiclassical models in Sections 2.1 and 2.2 provide an essentially exact description of the long time dynamics as $T \rightarrow 0$ for any fixed g , other than at the critical point $g = g_c$. As illustrated in Fig 1, this failure broadens into a wide quantum critical region at larger T , which is, in principle, easily accessible in experiments.

We begin our discussion of spin correlations in this region by first considering the single point $g = g_c$, $T = 0$. The energy gap vanishes here as $\Delta \sim |g - g_c|$. Also as $g \nearrow g_c$, the ferromagnetic order parameter vanishes¹⁴ as $N_0 \sim (g_c - g)^{1/8}$, and so it is not sensible anymore to think in terms of domain walls. Similarly, for $g \searrow g_c$, the quasiparticle residue vanishes¹¹ as $\mathcal{A} \sim (g - g_c)^{1/4}$, and so the flipped

spin quasiparticles are also not well defined at $g = g_c$. A less intuitive description of the long time dynamics must be developed here. The fundamental property of the critical point that enables a description of the dynamics is that of scale and conformal invariance. One signal of this invariance is the long distance behavior of the equal time σ^z correlation

$$\langle \sigma_j^z \sigma_k^z \rangle = \frac{Z}{|j - k|^{1/4}} \quad ; \quad g = g_c, \quad T = 0, \quad (11)$$

where Z is a non-zero, non-universal number. Remarkably, the powerful technology of conformal invariance allows one to reconstruct the exact long distance and long time spin correlation function at $T > 0$ using as input only the form (11) (such ‘wizardry’ is unfortunately not possible in higher dimensions). The answer is more easily expressed in terms of the dynamic susceptibility, $\chi(p, \omega)$, which is related to $S(p, \omega)$ in (4) by the usual fluctuation dissipation theorem:

$$\chi(p, \omega) = \left(\frac{\Gamma(7/8)c^{3/4}}{2^{7/4}\pi^{3/4}\Gamma(1/8)} \right) \frac{Z}{(k_B T/\hbar)^{7/4}} \frac{\Gamma\left(\frac{1}{16} - i\frac{\omega + cp}{4\pi k_B T/\hbar}\right) \Gamma\left(\frac{1}{16} - i\frac{\omega - cp}{4\pi k_B T/\hbar}\right)}{\Gamma\left(\frac{15}{16} - i\frac{\omega + cp}{4\pi k_B T/\hbar}\right) \Gamma\left(\frac{15}{16} - i\frac{\omega - cp}{4\pi k_B T/\hbar}\right)} \quad (12)$$

where c is the non-universal velocity of excitations at the critical point. This is a rather cumbersome expression whose functional form is not terribly intuitive. Its structure is nevertheless rather simple, and this becomes clear from the following expression which provides an excellent fit to (12) over a wide window of low frequencies or wavevectors (this is also the region over which the spectral density $\text{Im}\chi(p, \omega)/\omega$ has significant weight):

$$\chi(p, \omega) = \frac{\chi(0, 0)}{1 - i(\omega/\Gamma_R) + p^2\xi^2 - (\omega/\omega_1)^2}. \quad (13)$$

The relaxation rate Γ_R is given by

$$\begin{aligned} \Gamma_R &\equiv \left(i\chi(0, 0) \frac{\partial \chi^{-1}(0, \omega)}{\partial \omega} \Big|_{\omega=0} \right)^{-1} \\ &= \left(2 \tan \frac{\pi}{16} \right) \frac{k_B T}{\hbar} \end{aligned} \quad (14)$$

where we used (12) in the first equation. As claimed in the introduction, this characteristic frequency is a universal number times $k_B T/\hbar$. We determined ω_1 and ξ by fitting (13) to (12) over the range $0 < \omega, cp < 2k_B T/\hbar$ (the fit was essentially perfect) and obtained the best fit values

$$\omega_1 = 0.795k_B T/\hbar \quad ; \quad \xi = 1.280\hbar c/k_B T. \quad (15)$$

As expected, all time and length scales are determined by T alone. Notice that (13) has the structure of the response function of the conventional van Hove dynamics of an overdamped field.¹ What is novel here the characteristic damping frequency is not an adjustable phenomenological parameter depending upon the coupling to some heat bath, but a universal rate determined by the absolute temperature and fundamental constants of nature.

At large frequencies, $\hbar|\omega| \gg k_B T$, and wavevectors, $\hbar c|p| \gg k_B T$, the expression (12) reduces to

$$\chi(p, \omega) = \frac{\Gamma(7/8)2^{7/4}\pi c^{3/4}}{\Gamma(1/8)} \frac{Z}{(c^2 p^2 - \omega^2)^{7/8}} \quad (16)$$

This represents the spectrum at the gapless critical point $g = g_c$, $T = 0$; as expected, the complex frequency plane has no quasiparticle pole, but a branch-cut originating at $\omega = \pm cp$ associated with the continuum of critical excitations. For practical purposes, it is worth noting that the spectral weight in this critical region is rather small, and experimental observations at $T > 0$ will be dominated by the relaxation spectrum in (13).

3 Transition between BCS superconductors

This section reviews quantum critical dynamics in a two-dimensional model which may be of relevance to the cuprate high temperature superconductors. Observation¹⁵ of quantum critical behavior in the spectral function of the fermionic nodal quasiparticles stimulated our study^{16,17} of a wide class of possible models which could yield a suitable quantum critical point. It turned out to be rather difficult to satisfy the needed requirements: a quantum critical point below its upper critical dimension, with nodal quasiparticles a primary degree of freedom. Only two such candidates were found, both involving transitions with changes in the pairing symmetry of BCS superconductors in two dimensions: the transitions from a $d_{x^2-y^2}$ superconductor to either a $d_{x^2-y^2} + id_{xy}$ or a $d_{x^2-y^2} + is$ superconductor. We considered the first of these more likely on microscopic grounds and will review its theory here; the theory for the second is closely related. We also note that our interpretation of the spectra of the cuprates does not require that such a quantum phase transition be actually present on the physical axis as a function of doping; all that is required is that a quantum critical point be nearby in the generalized parameter space.

Recent tunnelling measurements¹⁸ have provided support for a transition from a $d_{x^2-y^2}$ superconductor at optimal doping to a $d_{x^2-y^2} + id_{xy}$ superconductor in the overdoped regime, at least in thin films of $Y_{1-y}Ca_yBa_2Cu_3O_{7-x}$. This sequence of transitions may be understood on the basis of some early theoretical work. While there is strong theoretical evidence for $d_{x^2-y^2}$ superconductivity in lightly doped antiferromagnets,¹⁹ studies of the Hubbard model in limit of very large hole density^{20,21} (low electron density) showed instead an instability to d_{xy} superconductivity. Interpolating between these limits, we can expect¹² that a $d_{x^2-y^2} + id_{xy}$ superconductor appears an intermediate phase.

As we are interested only in universal critical properties, we can develop a theory using the simplest phenomenological model which displays the required transition. So we consider the Hamiltonian

$$H_{tJ} = \sum_k \varepsilon_k c_{k\sigma}^\dagger c_{k\sigma} + J_1 \sum_{\langle ij \rangle} \mathbf{S}_i \cdot \mathbf{S}_j + J_2 \sum_{\text{nnn } ij} \mathbf{S}_i \cdot \mathbf{S}_j, \quad (17)$$

where $c_{j\sigma}$ is the annihilation operator for an electron on the square lattice site j with spin $\sigma = \uparrow, \downarrow$, $c_{k\sigma}$ is its Fourier transform to momentum space, ε_k is the

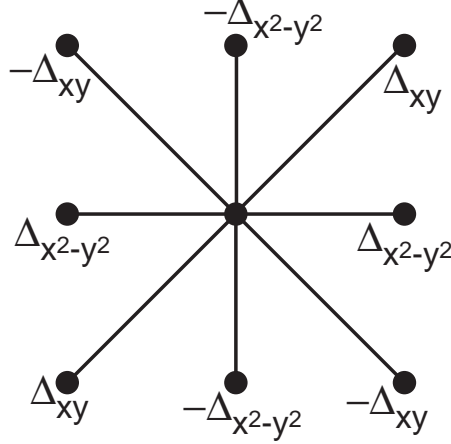


Figure 2. Values of the pairing amplitudes, $-\langle c_{i\uparrow}c_{j\downarrow} - c_{i\downarrow}c_{j\uparrow} \rangle$ with i the central site, and j is one of its 8 near neighbors.

dispersion of the electrons,

$$S_{j\alpha} = \frac{1}{2} c_{j\sigma}^\dagger \sigma_{\sigma\sigma'}^\alpha c_{j\sigma'} \quad (18)$$

with σ^α the Pauli matrices, and J_1, J_2 are first and second neighbor antiferromagnetic exchange interactions which induce the superconductivity. We apply the standard BCS theory to H_{tJ} : this will yield an adequate description of the low temperature properties, except in the vicinity of the quantum critical point. The BCS Hamiltonian is

$$H_{BCS} = \sum_k \varepsilon_k c_{k\sigma}^\dagger c_{k\sigma} - \frac{J_1}{2} \sum_{j,\mu} \Delta_\mu (c_{j\uparrow}^\dagger c_{j+\hat{\mu},\downarrow}^\dagger - c_{j\downarrow}^\dagger c_{j+\hat{\mu},\uparrow}^\dagger) + \text{h.c.} \\ - \frac{J_2}{2} \sum'_{j,\nu} \Delta_\nu (c_{j\uparrow}^\dagger c_{j+\hat{\nu},\downarrow}^\dagger - c_{j\downarrow}^\dagger c_{j+\hat{\nu},\uparrow}^\dagger) + \text{h.c.}, \quad (19)$$

where the first summation over μ is along the nearest neighbor directions \hat{x} and \hat{y} , while the second summation over ν is along the diagonal neighbors $\hat{x} + \hat{y}$ and $-\hat{x} + \hat{y}$. To obtain $d_{x^2-y^2}$ and d_{xy} pairing, we choose $\Delta_x = -\Delta_y = \Delta_{x^2-y^2}$, and $\Delta_{x+y} = -\Delta_{-x+y} = \Delta_{xy}$. We summarize our choices for the spatial structure of the pairing amplitudes (which determine the Cooper pair wavefunction) in Fig 2. The values of $\Delta_{x^2-y^2}$ and Δ_{xy} are to be determined by minimizing the ground state energy:

$$E_{BCS} = J_1 |\Delta_{x^2-y^2}|^2 + J_2 |\Delta_{xy}|^2 - \int \frac{d^2k}{4\pi^2} \left[\sqrt{\varepsilon_k^2 + |\Delta_k|^2} - \varepsilon_k \right] \quad (20)$$

where the pairing amplitude in momentum space is

$$\Delta_k = J_1 \Delta_{x^2-y^2} (\cos k_x - \cos k_y) + 2J_2 \Delta_{xy} \sin k_x \sin k_y. \quad (21)$$

Notice that the energy depends upon the relative phase of $\Delta_{x^2-y^2}$ and Δ_{xy} : this phase is therefore an observable property of the ground state.

The minimization of E_{BCS} was carried out in Ref. 12. For small J_2/J_1 the ground state was a $d_{x^2-y^2}$ superconductor with $\Delta_{x^2-y^2} \neq 0$ and $\Delta_{xy} = 0$. Above a critical value of J_2/J_1 there was a continuous transition to a state with $\Delta_{x^2-y^2} \neq 0$, $\Delta_{xy} \neq 0$, and

$$\arg(\Delta_{xy}) = \arg(\Delta_{x^2-y^2}) \pm \pi/2. \quad (22)$$

This is a $d_{x^2-y^2} + id_{xy}$ superconductor. The choice of the sign in (22) is associated with the breaking of time reversal symmetry, and this suggests that the transition can be described by a Z_2 Ising order parameter. As usual, we can associate the Ising order with a real, scalar field ϕ (the coarse-grained value of the local Ising order) which we can identify here by $\phi = i\Delta_{xy}$, in the gauge where $\Delta_{x^2-y^2}$ is real. However, the critical theory of the transition is *not* simply that of the quantum Ising model in 2+1 dimensions *i.e.* not that of the two-dimensional version of the model considered in Section 2. The fermionic quasi-particles are also primary critical degrees of freedom, and the required quantum field theory couples the Ising field ϕ to fermionic fields representing the lowest energy Bogoliubov quasiparticles. We will not explicitly write down this field theory here, and instead refer the reader to another recent review¹² by the author.

The finite temperature phase diagram of H_{tJ} in the vicinity of the critical point is sketched in Fig 3. We discuss below the nature of the fermion Green's function in the different regimes below the superconducting critical temperature T_c .

We can write the fermion Green's function in the superconductor compactly using the Nambu notation. We define the spinor field $\Psi_k = (c_{k\uparrow}, c_{-k\downarrow}^\dagger)$. Then the retarded Ψ_k Green's function $G(k, \omega)$ can be written as

$$\hbar G^{-1}(k, \omega) = \hbar\omega - \varepsilon_k \tau^z + \text{Re}(\Delta_k) \tau^x - \text{Im}(\Delta_k) \tau^y - \Sigma(k, \omega) \quad (23)$$

where $\tau^{x,y,z}$ are Pauli matrices in Nambu particle-hole space. The above expression follows from the BCS theory (19), with the self energy Σ representing the effects of interaction between the quasiparticles and any additional collective modes.

Consider first the low T region with $J_2 < J_{2c}$ in Fig 3. Here the ground state is well described by the BCS theory of the $d_{x^2-y^2}$ -wave superconductor. We can compute the effects of collisions between the fermionic quasiparticles in very much the same spirit as in Landau's Fermi liquid theory:³ the main difference is that instead of a whole Fermi surface, we now have isolated 'nodal' Fermi points at four points in the Brillouin zone determined by the solution of $\varepsilon_k = 0, \Delta_k = 0$. Consequently, the density of states for low-energy scattering of quasiparticles is even smaller than in a Fermi liquid, and the quasiparticles remain well-defined excitations. Right at the Fermi level, and at low T , these collisions lead to $\Sigma \sim iT^3$, which is smaller than the result $\sim iT^2$ in a conventional Fermi liquid. A quasiclassical description of the fermionic quasiparticles therefore remains valid, in the same framework used in Landau's Fermi liquid theory.

Next, we move to the opposite low T region in Fig 3 with $J_2 > J_{2c}$ and $d_{x^2-y^2} + id_{xy}$ superconductivity. Here time-reversal symmetry is broken with $\langle \phi \rangle \neq 0$. The theory of the quasiparticles is very similar to that in the small J_2 region above

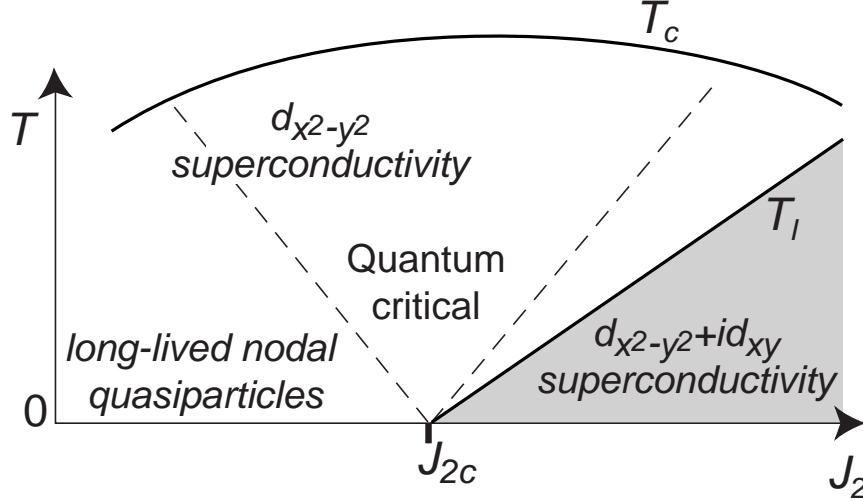


Figure 3. Phase diagram of $H_{t,J}$. As in Fig 1, dashed lines represent crossovers, but the full lines are true thermodynamic phase transitions. There is a quantum critical point at $T = 0$, $J_2 = J_{2c}$, but now it extends into a line of second order phase transitions at temperatures $T_I > 0$. The critical theory for the $T = 0$ quantum critical point was reviewed in Ref. 12 and involves an Ising field and fermionic degrees of freedom. The T_I line is in the universality class of the classical two-dimensional Ising model. The ground state is superconducting everywhere below T_c , with $d_{x^2-y^2} + id_{xy}$ superconductivity in the shaded region, and $d_{x^2-y^2}$ superconductivity elsewhere. The crossover boundaries and T_I approach the $T = 0$, $J_2 = J_{2c}$ critical point linearly because the best estimate^{22, 23} for the exponent $z\nu$ is 1.00.

with one very important difference. The equations $\varepsilon_k = 0, \Delta_k = 0$ now have no solution for any k and so the nodal points have been gapped out. There are still low-energy fermionic excitations near the position of the original nodal points, but these appear only above an energy gap Δ . As in Section 2, this energy gap vanishes as we approach the critical point as $\Delta \sim (J_2 - J_{2c})^{z\nu}$, and the best estimate^{22, 23} for the critical exponent is $z\nu \approx 1.00$. As long as $T \rightarrow 0$ at any fixed $\Delta > 0$, the density of thermally excited quasiparticles is exponentially small, and so $\Sigma \sim e^{-\Delta/T}$. So again a quasiclassical transport theory of the quasiparticle collisions applies.

Finally, we turn to the intermediate temperature quantum critical region in Fig 3, in the vicinity of the $J_2 = J_{2c}$ critical point. Here the physics is rather similar to the corresponding region in Section 2.3, but we no longer have the benefit of an exact solution for the spectral function. Strong fluctuations of the Ising order parameter ϕ , whose condensate gapped the nodal points in the $J_2 > J_{2c}$ region, now lead to strongly damped fermionic excitations. Loosely speaking, rapid temporal oscillations between $d_{x^2-y^2} + id_{xy}$ and $d_{x^2-y^2} - id_{xy}$ pairing lead to broad spectral functions. A theory for the low frequency form of the fermion spectral function was developed in Ref. 16, using an expansion in $(3 - d)$ (where d is the spatial dimensionality) and phenomenological ansatzes similar to (13) for the frequency and wavevector dependence of the spectral function of the critical excitations. At low frequencies near the Fermi level, the result can be written in the form (compare

(12) and (13))

$$G^{-1}(k, \omega) = Z^{-1} T^{\eta_f} (\hbar\omega - \varepsilon_k \tau^z + \Delta_k \tau^x + i\hbar\Gamma_R), \quad (24)$$

where η_f is a critical exponent, Z is a non-universal, non-singular prefactor, and we can take Δ_k real because $\langle \phi \rangle = 0$ in the quantum critical region. The estimates for the exponent η_f are $\eta_f \approx (3-d)/14$ in the $(3-d)$ expansion,¹⁶ and $\eta_f \approx 1/(3\pi^2 N)$, with $N = 2$, in the $1/N$ expansion.²² The damping rate Γ_R has the same remarkable universal structure we found in Section 2.3. Just as in (14), we now find^{16,22} that Γ_R is universally related to the absolute temperature, with

$$\Gamma_R = 0.581 \frac{k_B T}{\hbar} \quad (25)$$

in the $(3-d)$ expansion.

It is important to keep in mind that (24) is a low frequency form and does not hold at frequencies which are much larger than $k_B T/\hbar$. In the latter regime we obtain a result which is similar in structure to that obtained by taking the large ω limit of the exact result (12) of the quantum Ising chain. Near one of the nodal points we find

$$G(p, \omega) = Z C_f \frac{-\omega - c p_x \tau^z - c p_y \tau^x}{(c^2 p^2 - \omega^2)^{1-\eta_f/2}} \quad (26)$$

where p measures momentum deviation from one of the nodal points and the p co-ordinates have been rotated by 45 degrees from the k co-ordinates, C_f is a computable universal number, and c is a velocity. In principle the velocities appear before the τ^z and τ^x should be different, but they become equal in the asymptotic region near the critical point.¹⁶ The spectrum (26) is the analog of (16), and its most important property is, of course, that it does not have quasi-particle pole, but only a branch cut representing the continuum of critical excitations.

4 Disordered spin systems

The plethora of intermetallic “heavy fermion” compounds have provided a fertile ground for the study for the study of quantum phase transitions and the associated quantum critical region at finite temperature. Useful reviews of the current experimental and theoretical status have been provided recently by Coleman and collaborators.²⁴ Most of these systems are near a zero temperature magnetic ordering transition of some type, and this has allowed investigation of quantum criticality using a variety of probes. Among the most thoroughly investigated compounds is $\text{CeCu}_{6-x}\text{Au}_x$: neutron scattering and thermodynamic measurements²⁵ show convincing signs of universal critical behavior, with a characteristic frequency scale of order $k_B T/\hbar$ and scaling of dynamic response functions as a function of $\hbar\omega/k_B T$. This behavior is not compatible^{5,24} with spin-density wave theories,^{26,27} which consider perturbative corrections from interaction between collective paramagnon modes, and the search for the appropriate quantum-critical model is an active topic of current research. An important open question in these investigations is the importance of quenched disorder to the observed critical behavior. Theories for the onset of spin glass order in metallic systems have been proposed (see Ref. 28 for

a review), and glassy dynamics has been observed²⁹ in $\text{UCu}_{5-x}\text{Pd}_x$, a compound which also displays $\hbar\omega/k_B T$ scaling in neutron scattering.³⁰ More unexpectedly, the glassy behavior persists at compositions which are nominally stoichiometric³¹ ($x = 1$).

Here we shall review a class of theories which have their origin in studies of systems with strong quenched disorder. Analyses of disordered models of frustrated spin systems^{32,33} and doped Mott insulators³⁴ have shown that a useful starting point for the critical theory is a seemingly simple model which we shall describe below. It consists a single quantum spin interacting with a ‘bath’ of low energy collective spin excitations which represent a mean-field description of its environment. Generalized models have recently been argued to apply to systems in two dimensions even in the absence of quenched disorder.³⁵

We consider the following single spin quantum partition function, which defines a well-posed, quantum mechanical problem in its own right:

$$\mathcal{Z} = \int \mathcal{D}\mathbf{n}(\tau) \delta(\mathbf{n}^2(\tau) - 1) \exp \left(-iS \int_0^\beta A_\tau(\mathbf{n}(\tau)) d\tau + \int_0^\beta d\tau \int_0^\beta d\tau' D(\tau - \tau') \mathbf{n}(\tau) \cdot \mathbf{n}(\tau') \right). \quad (27)$$

Here τ is imaginary time which runs periodically from 0 to $\beta = \hbar/k_B T$, $\mathbf{n}(\tau)$ is the orientation of the quantum spin with $\mathbf{n}(\tau + \beta) = \mathbf{n}(\tau)$, and S its spin quantum number with $2S = \text{integer}$. The first term in \mathcal{Z} is the Berry phase of the spin, with $A_\tau(\mathbf{n}(\tau))d\tau$ equal to the area of the spherical triangle on the unit sphere with vertices at $\mathbf{n}(\tau)$, $\mathbf{n}(\tau + d\tau)$, and a fixed (but arbitrary) reference direction \mathbf{n}_0 . The function $D(\tau)$ (also periodic with period β) is the retarded self-interaction of the spin and represents the influence of the spin environment. The model \mathcal{Z} was introduced and examined in a large N expansion,³² and useful renormalization group analyses were presented.^{36,37} In its application as a mean-field theory of bulk lattice models, the solution of \mathcal{Z} usually has to be supplemented by a self-consistency condition for $D(\tau)$: the simplest of these is $D(\tau - \tau') = (J/\hbar)^2 \langle \mathbf{n}(\tau) \cdot \mathbf{n}(\tau') \rangle_{\mathcal{Z}}$, where J is an energy scale for the exchange interactions, but more complicated self-consistency conditions have also been considered.^{34,33,35}

In a quantum critical system, we may expect power-law correlations of all observables at $T = 0$. So it is of particular interest to examine \mathcal{Z} for the case where

$$D(\tau) \sim \frac{1}{|\tau|^{2-\alpha}} \quad (28)$$

for large $|\tau|$ at $T = 0$. Non-trivial spin correlations emerge for $\alpha > 0$, and the renormalization group analysis^{36,37} proceeds in powers of α . Although this is an interacting quantum field theory and it is not possible to compute the flow equations exactly, it was recently shown^{38,33} that the structure of the quantum theory allowed one to deduce some results to all orders in α ; in particular it was shown that for the case where $D(\tau)$ obeyed (28),

$$\langle \mathbf{n}(\tau) \cdot \mathbf{n}(\tau') \rangle_{\mathcal{Z}} \sim \frac{1}{|\tau - \tau'|^\alpha}. \quad (29)$$

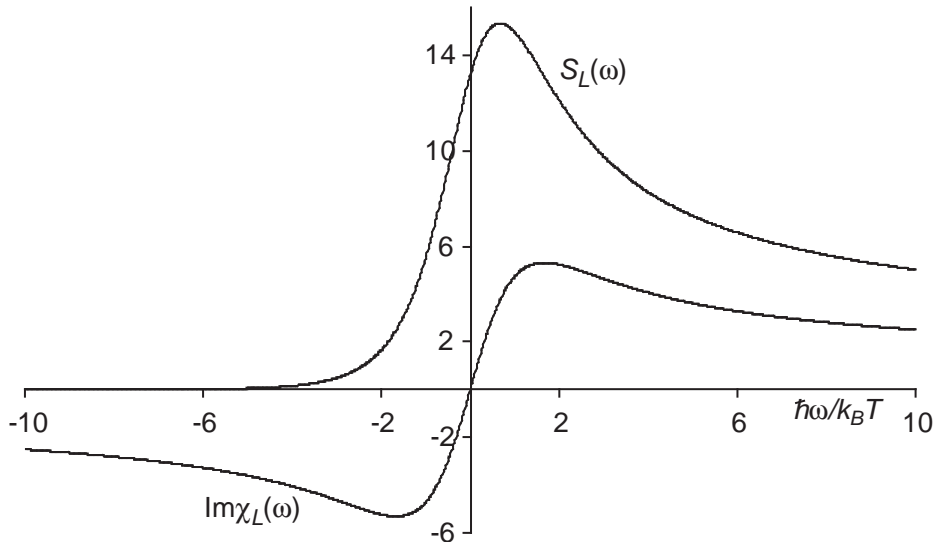


Figure 4. Plots of the dynamic local susceptibility $\text{Im}\chi_L(\omega)$, in (31), and the local dynamic structure factor (measured in neutron scattering experiments) $S_L(\omega) = 2\text{Im}\chi_L(\omega)/(1 - e^{-\hbar\omega/k_B T})$ at $\alpha = 1/2$ and some fixed temperature T . Note that $\text{Im}\chi_L(\omega)$ is an odd function of ω , while $S_L(\omega)$ is not an even function. At large $|\omega|$, $\text{Im}\chi_L(\omega) \sim \text{sgn}(\omega)/|\omega|^{1-\alpha}$.

This is a non-trivial result,^{32,36,37,38,33} and depends crucially on the the Berry phase term in \mathcal{Z} . Comparison of (29) and (28) with the particular self-consistency condition mentioned above selects the value $\alpha = 1$, and this is the value that has appeared frequently in physical applications.^{32,34,33,35}

The result (29) allows us to directly compute the observable local dynamic spin susceptibility, $\chi_L(\omega)$ in the quantum critical region; we define this quantity by the Fourier transform in imaginary frequency

$$\chi_L(i\omega_n) = \int_0^\beta d\tau e^{i\omega_n \tau} \langle \mathbf{n}(\tau) \cdot \mathbf{n}(\tau') \rangle_{\mathcal{Z}}. \quad (30)$$

While the result (29) is exact at $T = 0$ for the model obeying (28), the form of the exact result at $T > 0$ is not known. However, a solution for the $T > 0$ dynamics is possible in the large N limit;^{34,39} the right hand side of (29) is replaced by $[\pi T / \sin(\pi T |\tau - \tau'|)]^\alpha$, and its Fourier transform yields the result

$$\text{Im}[\chi_L(\omega)] \sim T^{\alpha-1} \sinh\left(\frac{\hbar\omega}{2k_B T}\right) \left| \Gamma\left(\frac{\alpha}{2} - i\frac{\hbar\omega}{2\pi k_B T}\right) \right|^2. \quad (31)$$

This constitutes the complete description of the relaxational quantum critical spin dynamics: note again that the function depends universally on $\hbar\omega/k_B T$. At the important value $\alpha = 1$, (31) reduces to the simple result $\text{Im}[\chi_L(\omega)] \sim \tanh(\hbar\omega/2k_B T)$. We show a plot of the spectral function (31) at $\alpha = 1/2$ in Fig 4.

The result (31) is also that expected if the local spin dynamics obeys a conformally invariant field theory in 1+1 dimensions.⁴⁰ There is no reason for this to be generally the case for \mathcal{Z} , and (31) has been shown to hold only in a large N limit; we expect corrections to the scaling function of ω/T at higher orders, and computing these remains an important challenge. Comparisons of (31) with experimental data on $\text{UCu}_{5-x}\text{Pd}_x$ have been made;^{40,41,42} while some higher frequency features are reasonably captured, the agreement is poor for $\hbar\omega \ll k_B T$, and it has been proposed that this is due to the effects of disorder.⁴²

5 Conclusions

We have presented here a series of paradigms of dynamic response functions at finite temperatures near a quantum critical point. The behavior discussed here is characteristic of critical points below their upper critical dimension. As the number and precision of experimental measurements of such critical points increases, we hope that the accuracy of theoretical predictions will be eventually be sufficient to permit a quantitative confrontation between theory and experiment.

We have not discussed here the dynamics of systems above their upper-critical dimension: in these cases the dynamics usually remains quasiclassical even near the critical point, and a van-Hove like theory with a relaxation rate dependent upon microscopic details provides an adequate description.

Acknowledgments

This research was supported by US NSF Grant DMR 0098226.

References

1. D. Forster, *Hydrodynamic Fluctuations, Broken Symmetry, and Correlation Functions*, Benjamin Cummings, Reading, Mass. (1975).
2. S. W. Lovesey, *Condensed Matter Physics, Dynamic Correlations*, Benjamin Cummings, Reading, Mass. (1980).
3. L. D. Landau and E. M. Lifshitz, *Statistical Physics*, Pergamon Press, Oxford (1980).
4. B. I. Halperin and P. C. Hohenberg, *Rev. Mod. Phys.* **49**, 435 (1977).
5. S. Sachdev, *Quantum Phase Transitions*, Cambridge University Press, Cambridge U.K. (1999).
6. S. Chakravarty, B. I. Halperin, and D. R. Nelson, *Phys. Rev. B* **39**, 2344 (1989).
7. S. Sachdev and J. Ye, *Phys. Rev. Lett.* **69**, 2411 (1992).
8. A. V. Chubukov, S. Sachdev, and J. Ye, *Phys. Rev. B* **49**, 11919 (1994).
9. S. Sachdev, *Phys. Rev. B* **59**, 14054 (1999).
10. K. Damle and S. Sachdev, *Phys. Rev. B* **56**, 8714 (1997).
11. S. Sachdev and A.P. Young, *Phys. Rev. Lett.* **78**, 2220 (1997).
12. S. Sachdev, cond-mat/0109419.
13. V. E. Korepin, N. M. Bogoliubov, and A. G. Izergin, *Quantum Inverse Scattering Method and Correlation Functions*, Cambridge University Press, Cam-

- bridge U.K. (1993).
14. P. Pfeuty *Ann. of Phys.* **57**, 79 (1970).
 15. T. Valla, A. V. Fedorov, P. D. Johnson, B. O. Wells, S. L. Hulbert, Q. Li, G. D. Gu, and N. Koshizuka, *Science* **285**, 2110 (1999).
 16. M. Vojta, Y. Zhang, and S. Sachdev, *Phys. Rev. B* **62**, 6721 (2000).
 17. M. Vojta, Y. Zhang, and S. Sachdev, *Phys. Rev. Lett.* **85**, 4940 (2000).
 18. Y. Dagan and G. Deutscher, *Phys. Rev. Lett.* in press, cond-mat/0106128.
 19. C. J. Halboth and W. Metzner *Phys. Rev. Lett.* **85**, 5162 (2000).
 20. M. A. Baranov and M. Yu Kagan, *Z. Phys. B* **86**, 237 (1992).
 21. M. A. Baranov, A. V. Chubukov, and M. Yu Kagan, *Int. J. Mod. Phys. B* **6**, 2471 (1992).
 22. D. V. Khveshchenko and J. Paaske, *Phys. Rev. Lett.* **86**, 4672 (2001).
 23. L. Kärkkäinen, R. Lacaze, P. Lacock, and B. Petersson, *Nucl. Phys. B* **415**, 781 (1994).
 24. P. Coleman, C. Pepin, Q. Si, and R. Ramazashvili, *J. Phys. C (Cond. Matt.)* **13**, 723, (2001); P. Coleman and C. Pepin, cond-mat/0110063.
 25. A. Schröder, G. Aeppli, R. Coldea, M. Adams, O. Stockert, H.v. Löhneysen, E. Bucher, R. Ramazashvili, and P. Coleman, *Nature* **407**, 351 (2000).
 26. J. A. Hertz, *Phys. Rev. B* **14**, 1165 (1976).
 27. A. J. Millis, *Phys. Rev. B* **48**, 7183 (1993).
 28. S. Sachdev, *Phil. Trans. Roy. Soc. London A* **356**, 173 (1998).
 29. D. E. MacLaughlin, O. O. Bernal, R. H. Heffner, G. J. Nieuwenhuys, M. S. Rose, J. E. Sonier, B. Andraka, R. Chau, and M. B. Maple, *Phys. Rev. Lett.* **87**, 066402 (2001).
 30. M. C. Aronson, R. Osborn, R. A. Robinson, J. W. Lynn, R. Chau, C. L. Seaman, and M. B. Maple, *Phys. Rev. Lett.* **75**, 725 (1995).
 31. D. E. MacLaughlin, R. H. Heffner, G. J. Nieuwenhuys, G. M. Luke, Y. Fudamoto, Y. J. Uemura, R. Chau, M. B. Maple, and B. Andraka, *Phys. Rev. B* **58**, R11849 (1998).
 32. S. Sachdev and J. Ye, *Phys. Rev. Lett.* **70**, 3339 (1993).
 33. A. Georges, O. Parcollet, and S. Sachdev, *Phys. Rev. Lett.* **85**, 840 (2000); *Phys. Rev. B* **63**, 134406 (2001).
 34. O. Parcollet and A. Georges, *Phys. Rev. B* **59**, 5341 (1999).
 35. Q. Si, S. Rabello, K. Ingersent, and J. L. Smith, cond-mat/0011477.
 36. A. M. Sengupta, *Phys. Rev. B* **61**, 4041 (2000).
 37. J. L. Smith and Q. Si, *Europhys. Lett.* **45**, 228 (1999).
 38. M. Vojta, C. Buragohain, and S. Sachdev, *Phys. Rev. B* **61**, 15152 (2000).
 39. O. Parcollet, A. Georges, G. Kotliar, and A. M. Sengupta, *Phys. Rev. B* **58**, 3794 (1998).
 40. M. C. Aronson, M. B. Maple, P. de Sa, A. M. Tsvelik, and R. Osborn, *Europhys. Lett.* **40**, 245 (1997).
 41. M. C. Aronson, M. B. Maple, R. Chau, A. Georges, A. M. Tsvelik, and R. Osborn, *J. Phys. C (Cond. Matt.)* **8**, 9815 (1996).
 42. R. Chau, M. C. Aronson, E. J. Freeman, and M. B. Maple, *J. Phys. C (Cond. Matt.)* **12**, 4495 (2000).